



SiPM response to long and intense light pulses



S. Vinogradov^{a,b,*}, A. Arodzero^{c,d}, R.C. Lanza^c, C.P. Welsch^a

^a University of Liverpool and Cockcroft Institute, Sci-Tech Daresbury, Keckwick Lane, Warrington WA4 4AD, UK

^b P.N. Lebedev Physical Institute of the Russian Academy of Sciences, 119991 Leninskiy prospekt 53, Moscow, Russia

^c Department of Nuclear Science and Engineering, Massachusetts Institute of Technology, 77 Massachusetts Ave., Cambridge, MA 02139, USA

^d RadiaBeam Technologies Inc., 1717 Stewart St., Santa Monica, CA 90404, USA

ARTICLE INFO

Available online 3 December 2014

Keywords:

Silicon photomultiplier
SiPM
Scintillation
Cherenkov
Transient
Nonlinearity

ABSTRACT

Recently Silicon Photomultipliers (SiPMs) have become well recognized as the detector of choice for various applications which demand good photon number resolution and time resolution of short weak light pulses in the nanosecond time scale. In the case of longer and more intensive light pulses, SiPM performance gradually degrades due to dark noise, afterpulsing, and non-instant cell recovering. Nevertheless, SiPM benefits are expected to overbalance their drawbacks in applications such as X-ray cargo inspection using Scintillation-Cherenkov detectors and accelerator beam loss monitoring with Cherenkov fibres, where light pulses of a microsecond time scale have to be detected with good amplitude and timing resolution in a wide dynamic range of 10^5 – 10^6 .

This report is focused on transient characteristics of a SiPM response on a long rectangular light pulse with special attention to moderate and high light intensities above the linear dynamic range. An analytical model of the transient response and an initial consideration of experimental results in comparison with the model are presented.

© 2014 Elsevier B.V. All rights reserved.

1. Introduction

In the last decade Silicon Photomultipliers (SiPMs) have become well recognized as very competitive photodetectors due to their unique photon number resolution at room temperature, exceptional single photon time resolution, low operating voltages, compactness, and insensitivity to magnetic fields. Detection of short weak light pulses of nanosecond time scale appears to be the best suited for SiPM applications because for these signals most of the SiPM drawbacks have rather limited effect on the amplitude and time resolution of the signal. For these reasons, the most popular applications of SiPM technology are short-decay scintillation and Cherenkov light detection in high energy physics (particle calorimeters, Cherenkov telescopes, and imaging arrays) and in nuclear medicine (gamma cameras, positron emission tomography systems, namely PET/MRI, TOF-PET scanners) [1,2]. These applications require only very limited information to be extracted from a photodetector output signal: the number of photons and/or arrival time of the light pulse, and nothing else, because the pulse shape is not a subject of measurement.

In the case of detecting relatively long pulses starting from the microsecond time scale, the SiPM performance in photon number resolution is considerably affected by noise contributions from afterpulsing and dark counts as well as by losses of the detected photons due to non-instant cell recovery and a limited number of cells. Detection of arbitrary waveform light signals in order to reconstruct an input signal temporal structure from an output seems to be an especially challenging application for SiPM. At very low light intensity SiPM should be competitive with mature photon counters of much higher photon detection efficiency and much lower dark count rate (e.g. PMT and Geiger mode APD). At high light intensity SiPM should be competitive with a variety of conventional photodetectors (e.g. linear mode APD and PIN) of much higher photon detection efficiency, much wider dynamic range, and higher bandwidth. Nevertheless, there are some mixed applications which demand arbitrary signal waveform detection with photon number resolution where SiPM is expected to be more beneficial than other photodetectors.

X-ray cargo inspection with Scintillation-Cherenkov detectors is one such challenging application because good amplitude and timing resolution of a temporal structure of a light signal is required to reconstruct an absorption profile inside a cargo under test [3–5]. In such inspection systems, the intensities of scintillation and Cherenkov signals in detectors can vary by as much as 1:100,000 due to highly variable X-ray absorption inside the cargo (Figs. 1, 2).

* Corresponding author at: University of Liverpool and Cockcroft Institute, Sci-Tech Daresbury, Keckwick Lane, Warrington WA4 4AD, UK.
Tel.: +44 19 25 60 31 97; fax: +44 19 25 86 42.

E-mail address: Sergey.Vinogradov@liverpool.ac.uk (S. Vinogradov).

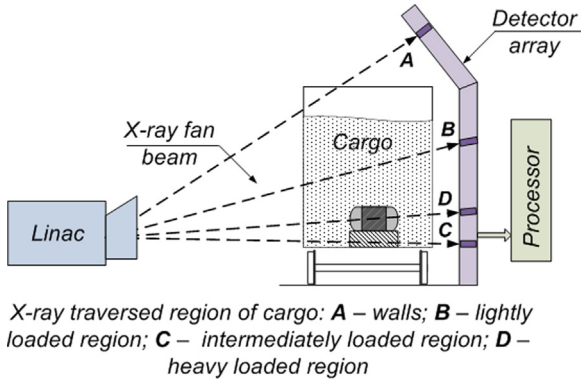


Fig. 1. Scheme of an X-ray accelerator-based cargo inspection system. As a result of a wide range of attenuation paths, the detector output signal intensities can vary by as much as 100,000 to one (reproduced from [5]).

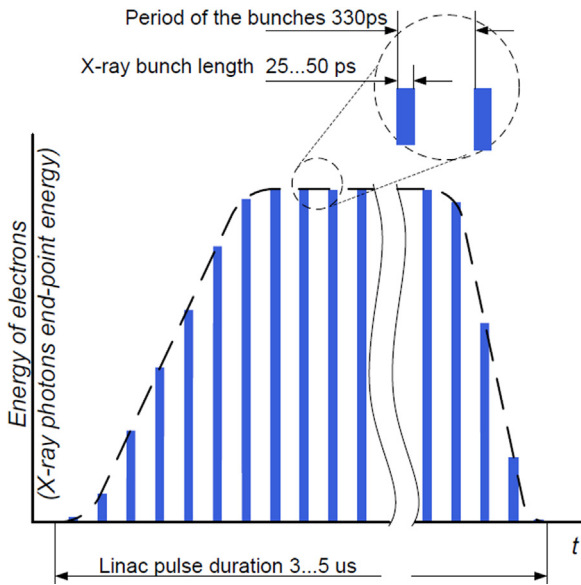


Fig. 2. X-ray pulse produced by typical Linac-based source. Several microseconds duration pulse consists of bunches of X-ray micro-pulses, about 25...50 ps duration each with period about 330 ps (reproduced from [5]).

An initial analysis for the possible application of SiPM (MPPC) in a cargo accelerator-based inspection system has been presented in our earlier report [5]. This report was focused on energy resolution with a special attention to SiPM nonlinearity and saturation effects.

Accelerator beam loss monitoring (BLM) using a Cherenkov fibre and SiPM readout (Fig. 3) is another application with arbitrary waveform light signals of very wide dynamic range ($\sim 10^6$) from a few Cherenkov photons up to a few percent fraction of destructive losses in an accelerator [6,7]. Light pulse shape at the fibre output is in general unpredictable as it reflects the location of beam losses in about 100 m long Cherenkov fibre placed in parallel with the beam line. The main goal of the detection is to reconstruct initial light intensity profile to identify beam loss location profile alongside the beam line resolving the number of lost particles per location (Fig. 4).

This report is focused on the SiPM response dynamics and transient characteristics for the long light pulse detection ($T_{\text{pulse}} > T_{\text{rec}}$, where T_{pulse} is a light pulse duration, and T_{rec} is a cell recovery time). Special attention has been paid to high light intensities approaching to SiPM saturation level. It would be worth to note that such a case has been out of scope for most SiPM studies up to now except just a few examples [8].

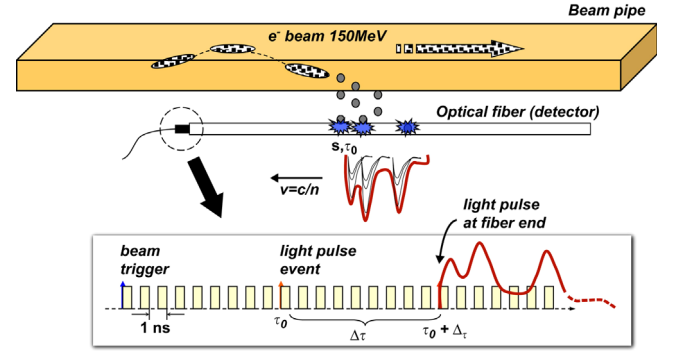


Fig. 3. Beam Loss Monitoring schematic: a beam line with relativistic electrons, Cherenkov optical fibre with Cherenkov photon detector (MPPC) at the upstream fibre end, and input/output pulse timing profiles (reproduced from [6]).

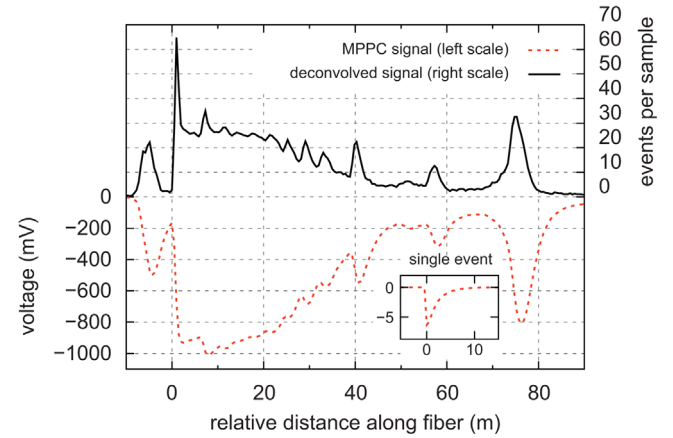


Fig. 4. MPPC output response at the BLM: raw MPPC signal (dashed line, left scale) and after deconvolution with single electron pulse shape (solid line, right scale) (reproduced from [6]).

2. Method

2.1. Experiment

Experiments have been carried out with rectangular pulses (8 ns rise & fall times) of 440 nm from an LED with variable intensity, repetition rate, and pulse width (nanosecond to microsecond time scale range). The light illuminated over the MPPC was uniformly distributed. The SiPM light response was read out without a preamplifier to avoid any possible nonlinearities and saturation at high output signal level. The SiPM anode was directly connected to a 50 Ω oscilloscope input of DC to 1 GHz analogue bandwidth and grounded through 50 Ω inside an acquisition box for an appropriate coupling.

For calibration of an output signal in single electron response (SER) units, the SER amplitudes have been measured with 20 dB, 4 GHz external amplifier Mini-Circuits ZX60-4016E+.

Hamamatsu MPPC S10362-33-050 C 3×3 mm² of 50 μ m cell size has been used as a well-known and very popular representative of SiPM technology.

2.2. Model

To the best of our knowledge, there are no models for arbitrary waveform detection by SiPMs except some Monte Carlo simulations and electrical circuit models [9,10]. However, SiPM performance in photon number and time resolution in the case of short pulse detection is comprehensively modelled due to its high practical importance [11,12], but results have rather limited applicability to

an arbitrary waveform case. Indeed, a variety of correlated effects: crosstalk, afterpulsing, and nonlinearity due to pixel recovering and limited number of pixels should be considered as dependent transient processes. Therefore, the statistics of SiPM output events depends on the history of previous detections and on signal intensity, in contrast with rather simple Poisson point process statistics for incident photon flux.

These complications motivate us to utilize an SiPM model [13] which combines contributions of all essential effects pointed above and at the same time provides reasonable simple analytical expressions for SiPM response in terms of the probability distribution of detected photons. However, the model results have been rewritten in terms of a transient photon counting process, and the light pulse shape is assumed to be rectangular for clarity and simplicity of analysis and instrumentation.

At the initial stage ($0 \leq t < T_{\text{rec}}$) a number of fired cells follow a binomial distribution model:

$$N_{\text{bin}}(t) = N_{\text{cell}} \times \left[1 - \exp\left(-\frac{I_{\text{ini}} \times t}{N_{\text{cell}}}\right) \right]$$

$$I_{\text{bin}}(t) = \frac{dN_{\text{bin}}(t)}{dt} = I_{\text{ini}} \times \exp\left(-\frac{I_{\text{ini}} \times t}{N_{\text{cell}}}\right)$$

$$I_{\text{ini}} = I_{\text{ph}} \times PDE \times (1 + n_{\text{ct}}), \quad (1)$$

Where $N_{\text{bin}}(t)$ and $I_{\text{bin}}(t)$ are the mean number and count rate of fired cells, I_{ini} is a potential count rate of electrons capable to initiate the firing of cells, N_{cell} is the total number of cells, I_{ph} is an incident photon rate, PDE is the photon detection efficiency, and n_{ct} is the mean number of crosstalk events per single primary event. So, the dynamics of an initial stage is an exponential decay of output signal $I_{\text{bin}}(t)$ with characteristic time $N_{\text{cell}}/I_{\text{ini}}$, which reflects photon detection losses due to the decreasing number of cells available for firing.

The intermediate stage of detection ($t \sim T_{\text{rec}}$) is a mixture of the tail from binomial decay and the initial recovery of the first

portion of fired cells. It would be difficult to describe this with a reasonably simple analytical model.

The final stage of detection ($t \gg T_{\text{rec}}$) is governed by a steady-state process with a balance between repetitive retriggering and recovering of SiPM cells, which can be described by a non-paralizable dead time model well known for Geiger counters. The model predicts an approximately Gaussian distribution of photon detection events with a constant mean count rate I_{steady} :

$$I_{\text{steady}} = \frac{I_{\text{ini-st}}}{1 + \frac{I_{\text{ini-st}} \times T_{\text{rec}}}{N_{\text{cell}}}}$$

$$\times I_{\text{ini-st}} = I_{\text{ini}} \times (1 + n_{\text{ap}}), \quad (2)$$

Where $I_{\text{ini-st}}$ is a steady-state potential count rate taking into account an afterpulsing contribution with a mean number of afterpulses n_{ap} per single primary event.

The total output signal may be roughly approximated by the sum of the binomial and steady-state components because both of them co-exist at any stage of the long pulse detection (losses of photon hits into already fired cells due to limited number of cells as well as losses due to the non-instant recovery process).

3. Results on SiPM response dynamics

The output response from a MPPC using a long rectangular light pulse ($T_{\text{pulse}} \gg T_{\text{rec}}$) reveals rather complicated transient behaviour. A set of typical responses are shown on Fig. 5.

The response from a very low intensity photon flux is a series of random SER pulses with some excess events due to crosstalk and afterpulsing, and this well-known case has been out of the scope of our study. Increasing the light intensity results in the overlapping of SER pulses yet providing, on average, a rectangular output pulse. However, this overlapping does not mean the overloading of

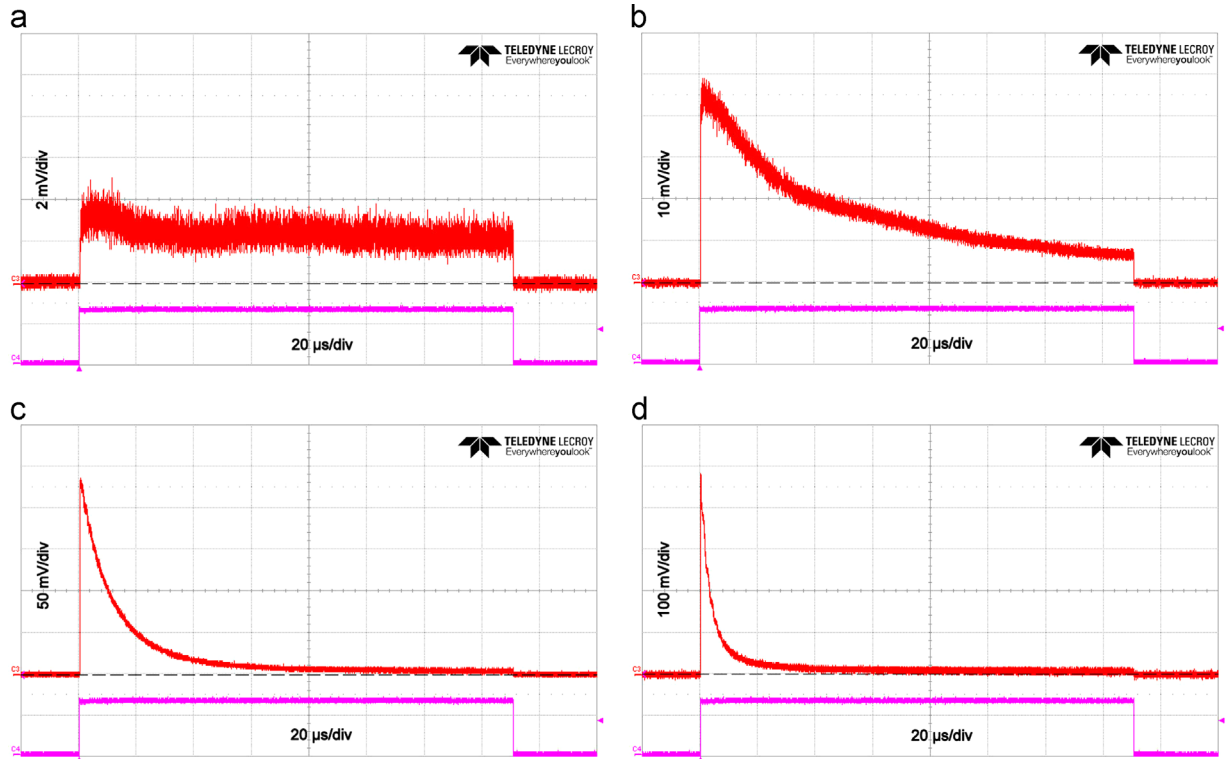


Fig. 5. Direct readout from Hamamatsu MPPC S10362-33-050 C (50 μm cell size, $3 \times 3 \text{ mm}^2$ area) without amplifier in an analogue bandwidth from DC to 1 GHz (upper traces) in response to a 150 μs rectangular LED pulse (lower traces) of variable intensity: cell loads L are 0.24 phe/cell (a), 0.44 phe/cell (b), 1.1 phe/cell (c), and 4.3 phe/cell (d). The vertical scales are 2 mV/div (a), 10 mV/div (b), 50 mV/div (c), and 100 mV/div (d). The horizontal scale is 20 μs /div for all plots.

individual cells. For the MPPC S10362-33-050 C with $N_{\text{cell}}=3600$ and with the SER decay time equal to the cell recovery time $T_{\text{rec}} \approx 30$ ns, the overlapping starts at a count rate of about 30 Mcps. In this case a cell load L defined as a number of photoelectrons or potential firings during T_{rec} is very low: $L = I_{\text{ini}} \cdot T_{\text{rec}} / N_{\text{cell}} \approx 2.8 \cdot 10^{-4}$ [phe/cell].

At an intermediate light intensity, where is a lower bound of an area of our interest, the MPPC output is almost rectangular with slightly pronounced initial decay (Fig. 5a; $L=0.24$). At higher light intensities the response has a more pronounced exponential decay with longer characteristic time as well as more relatively depressed steady-state plateau at the final stage (Figs. 5b, c, and d; $L=0.44$, 1.1, and 4.3 correspondingly).

4. Discussion

According to expressions (1), the initial stage of the SiPM output response on rectangular light pulse should be an exponential decay with a characteristic time inversely proportional to the peak amplitude. This dependence is presented on Fig. 6, which shows good correspondence of a hyperbolic trend line with the experimental results.

However, it would be much more valuable if the model could be applicable to describe the whole output signal including the steady-state plateau at the final stage.

In order to check this opportunity the total output signal may be roughly approximated by the sum of the binomial (1) and steady-state components (2) despite lacking a description for an intermediate stage, we assume a seamless coupling of the expressions makes sense because both of the components co-exist at any stage of the long pulse detection (losses of photon hits into unrecovered cells due to limited number of cells as well as losses due to non-instant recovery process).

The comparison of a joint signal approximation and typical experimental data is shown in Fig. 7 for medium load ($L=0.66$). In spite of a good fit at the initial stage, the first model plot related to well-known MPPC recovery time value $T_{\text{rec}}=30$ ns diverges at the final stage.

We have identified several clear reasons for why this may happen. First, an initial detection process is firmly governed by a binomial distribution of initiating electrons of any origin into ready-to-be-fired cells. A single adjustable parameter of the process I_{ini} is fixed during the initial stage because photon detection and crosstalk of subnanosecond time scale are instant processes at microsecond time scale; and recovery process a fortiori afterpulsing are negligible. Dynamics of the intermediate stage is considerably affected by transients of the aforementioned processes until the inevitable final steady-state. And again, the steady-state level is more or less fixed by a balance between the same initiating electron rate with additional contribution from afterpulsing $I_{\text{ini-st}}$ and a rate of cell recovering.

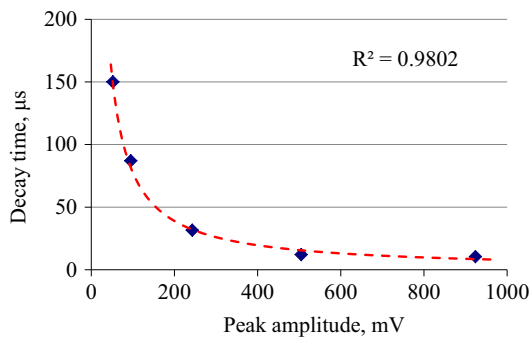


Fig. 6. Experiment and binomial model of SiPM response characteristics for initial stage: observing an inverse proportionality of the initial decay time and initial peak amplitude.

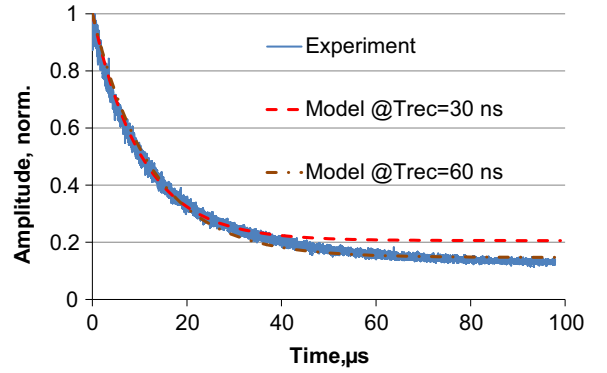


Fig. 7. Experiment and joint approximation model of SiPM transients (see Discussion for details).

Thus, intermediate and final stages are very sensitive to the recovery process dynamics and the value of T_{rec} while any contribution from afterpulsing is rather limited and could not exceed typically 10%–15%. Indeed, the second model plot calculated with the assumption of $T_{\text{rec}}=60$ ns is much closer to the experimental data. This could be caused by a dependence on the characteristic recovery time of the number of fired cells as expressed in [14]. According to this model for the S10362-33-050 C MPPC at saturation, we estimate that T_{rec} could be up to 53% higher than that for a single fired cell, thus this effect should be observed as a transient elongation of T_{rec} with a gradual decrease of the plateau level I_{steady} during detection. Any kind of non-exponential (bi-exponential) decay dynamics with some hidden slow component of recovery process could considerably affect the result as well.

Authors have also been advised that another possible source of less predictable behaviour of SiPM could be a thermal heating of microcells under repetitive firing during long pulse detection of high intensity [15]. In fact, the increase of temperature of avalanche junctions results in a shift of breakdown voltage to higher values, lowering overvoltage and suppression of gain and PDE, that is, transient lowering of an output signal in a microsecond time scale. Obviously, this effect should be clarified in more detail.

5. Conclusion

The SiPM response on a long rectangular light pulse reveals a complex transient behaviour with a strong dependence on the light intensity with respect to the total number of cells and cell recovery time. Nevertheless, a rather simple analytical model provides an acceptable approximate description of the SiPM dynamics using a sum of contributions from binomial and recovery time related losses of detected photons.

Arbitrary waveform signal detection is a very challenging application for any existing SiPM because of high distortion of an output pulse shape at high light intensities. Hopefully, this issue could be eliminated by a new generation of high density, fast recovery, fast response, low crosstalk, and low afterpulsing SiPMs which are under ongoing developments.

Acknowledgement

This work has been supported in part by the EC under Grant Agreement 329100 and the STFC Cockcroft Institute Core Grant No ST/G008248/1. This work also has been supported in part by the US Department of Homeland Security, Domestic Nuclear Detection Office, under competitively awarded contract IAA HSHQDC-13-C-B0019. This

support does not constitute an express or implied endorsement on the part of the US Government.

References

- [1] P. Buzhan, B. Dolgoshein, L. Filatov, A. Ilyin, V. Kantzerov, V. Kaplin, et al., Silicon photomultiplier and its possible applications, *Nucl. Instrum. Meth. A* 504 (2003) 48–52. [http://dx.doi.org/10.1016/S0168-9002\(03\)00749-6](http://dx.doi.org/10.1016/S0168-9002(03)00749-6).
- [2] G. Llosá, Overview of multicell geiger-mode avalanche photodiodes (SiPM) applications, *International Workshop on New Photon-detectors (PhotoDet, Orsay, France, 2012)*.
- [3] A. Arodzero, M. Rommel, A. Saverskiy, R. Sud, System and methods for intrapulse multi-energy and adaptive multi-energy X-ray cargo inspection. US Patent No. 8,457,274.
- [4] A. Arodzero, Scintillation-Cherenkov detector and method for high-energy X-ray cargo container imaging and industrial radiography, US Patent Application No. US 2011/0163236.
- [5] S. Vinogradov, A. Arodzero, R.C. Lanza, Performance of X-ray detectors with SiPM readout in cargo accelerator-based inspection systems, in: *IEEE Nucl. Sci. Symp. Med. Imaging Conf. (2013 NSS/MIC)*, IEEE, 2013, 1–6. 10.1109/NSSMIC.2013.6829597.
- [6] D. Di Givonale, L. Catani, L. Fröhlich, A read-out system for online monitoring of intensity and position of beam losses in electron linacs, *Nucl. Instrum. Meth. Phys. Res. A* 665 (33–39) (2011), <http://dx.doi.org/10.1016/j.nima.2011.11.038>.
- [7] L.J. Devlin, C.P. Welsch, E.N. del Busto, Update on Beam Loss Monitoring at CTF3 for CLIC, IBIC 2013, Oxford, UK, 2013.
- [8] M. Caccia, A. Bulgheroni, C. Cappellini, V. Chmill, M. Ramilli, F. Risigo, Response of silicon photo-multipliers to a constant light flux, *Nucl. Phys. B-Proc. Sup.* 197 (30–34) (2009), <http://dx.doi.org/10.1016/j.nuclphysbps.2009.10.028>.
- [9] P. Eckert, R. Stamen, H.-C. Schultz-Coulon, Study of the response and photon-counting resolution of silicon photomultipliers using a generic simulation framework, *J. Instrum.* (2012), <http://dx.doi.org/10.1088/1748-0221/7/08/P08011> (P08011–P08011).
- [10] D. Marano, G. Bonanno, M. Belluso, S. Billotta, A. Grillo, S. Garozzo, et al., Improved SPICE electrical model of silicon photomultipliers, *Nucl. Instrum. Meth. A* 726 (1–7) (2013), <http://dx.doi.org/10.1016/j.nima.2013.05.127>.
- [11] H.T. van Dam, S. Seifert, R. Vinke, P. Dendooven, H. Lohner, F.J. Beekman, et al., A comprehensive model of the response of silicon photomultipliers, *IEEE T. Nucl. Sci.* 57 (2010) 2254–2266. <http://dx.doi.org/10.1109/TNS.2010.2053048>.
- [12] S. Seifert, H.T. van Dam, R. Vinke, P. Dendooven, H. Lohner, F.J. Beekman, et al., A comprehensive model to predict the timing resolution of SiPM-based scintillation detectors: theory and experimental validation, *IEEE T. Nucl. Sci.* 59 (190–204) (2012), <http://dx.doi.org/10.1109/TNS.2011.2179314>.
- [13] S. Vinogradov, et al., Efficiency of solid state photomultipliers in photon number resolution, *IEEE T. Nucl. Sci.* 58 (2011) 9–16.
- [14] D. Marano, M. Belluso, G. Bonanno, S. Billotta, A. Grillo, S. Garozzo, et al., Silicon photomultipliers electrical model extensive analytical analysis, *IEEE T. Nucl. Sci.* 61 (23–34) (2014), <http://dx.doi.org/10.1109/TNS.2013.2283231>.
- [15] S. Dolinsky, Private Commun. July 2014.